


# Synthesis and characterization of antipyrine-imprinted polymers and their application for sustained release

Archana Kushwaha<sup>1</sup> · Smita Singh<sup>1</sup> · Neha Gupta<sup>1</sup> ·  
Ambareesh Kumar Singh<sup>1</sup> · Meenakshi Singh<sup>1</sup> 

Received: 2 September 2017 / Revised: 17 February 2018 / Accepted: 27 March 2018 /

Published online: 2 April 2018

© Springer-Verlag GmbH Germany, part of Springer Nature 2018

**Abstract** In view of technological significance of molecularly imprinted polymers (MIPs) in drug delivery, the ‘grafting from’ approach was employed to develop surface-imprinted silica particles for selective recognition and sustained delivery of a pharmaceutical drug antipyrine (ANP). ANP–MIP was fabricated using methacrylic acid (MAA) as functional monomer and ethylene glycol dimethacrylate (EGDMA) as cross-linker by UV irradiation via iniferter approach. Voltammetric measurements was used to scale the extraction and rebinding of ANP on glassy carbon electrode with Pt wire as counter electrode, Ag/AgCl as reference electrode. Various parameters were optimized for ascertaining the performance of ANP–MIP such as time, temperature, and pH. Grafted MIP was characterized by FTIR, thermogravimetry, elemental analysis, surface morphology (AFM) besides the recognition, rebinding and selectivity studies. Calibration curve linearly increases in concentration range of 0.1–2.0 mM with correlation coefficient  $R^2 = 0.976$  and limit of detection (LOD) as  $0.448 \mu\text{g mL}^{-1}$ . Thus, fabricated ANP–MIP was studied for controlled release of drug under varying conditions.

**Keywords** Molecular imprinting · Surface-imprinted polymer · Iniferter · Antipyrine · Controlled release

**Electronic supplementary material** The online version of this article (<https://doi.org/10.1007/s00289-018-2326-x>) contains supplementary material, which is available to authorized users.

✉ Meenakshi Singh  
meenakshi@bhu.ac.in; meenakshibhu70@gmail.com

<sup>1</sup> Department of Chemistry, MMV, Banaras Hindu University, Varanasi 221005, India

## Introduction

Phenazone was the first synthetic analgesic drug, patented as trademark name, antipyrine (ANP). It is a non-steroidal anti-inflammatory drug used in testing the effects of other drugs or diseases on drug-metabolizing enzymes in the liver [1]. It is often used in combination with benzocaine to relieve pain and inflammation in ear and to remove build-up of earwax [2]. Recently, their significant role in management of acute migraine pain is recognized and is kept under level C medications (“possibly effective medication”) for it [3]. Wide usage of ANP and unsafe disposal of such drugs along with their metabolites to natural water bodies are polluting various segments of environment. As per the reports, ANP and its metabolites were found to contaminate municipal sewage effluents, ground water, drinking water, etc. [4–7]. As it is reported to cause toxic epidermal necrolysis, confluent exanthema, oedema of lips and eyelids, to limit the extraneous use of it, controlled and targeted delivery is necessitated at many instances to reduce their detrimental effects. The optimum drug delivery carrier should be synchronized with the physiological status of the patient and should provide a drug in response to changing intracorporeal environment [8].

As Lulinski highlights, MIPs could be a group of materials that have great potential in drug delivery for modern pharmacotherapy [9]. Molecular imprinting involves positioning functional monomers around the template molecules by covalent/non-covalent interaction followed by polymerization and extraction of template molecules from polymeric matrix. This approach creates template-shaped cavities in polymer matrices with memory of template molecules to be used in molecular recognition. Due to their tailor-made recognition sites for target analytes, intrinsic robustness, low cost and extensive lifetime, MIPs have already been identified as effective alternatives for the natural receptors in chemical assays or sensors [10–14]. Here, antipyrine-imprinted polymers are synthesized and studied for controlled release of ANP. Controlled release of ANP from mesoporous carbon was studied by Saha et al. [15], from mesoporous silica by Salonen et al. [16], from functionalized mesoporous silica by Goscianska et al. [17] and from hydrophilic polymer shells by Sangalli et al. [18–21]. This study is the first one to study controlled release of ANP from imprinted matrix. Imprinting of aminoantipyrine through bulk imprinting was reported by Yang et al. [22], but till now surface imprinting via iniferter approach for any ANP derivative is not reported yet. Living polymerization via ‘iniferter’ is particularly used by polymer fraternity as a single molecule acts as initiator, as transfer agent as well as a terminating agent. Usually dithiocarbamates are used as excellent iniferter agents. Here they are used to graft imprinting matrix on surface of silica particles via ‘grafting from’ approach. Silica particles were modified by silanization with 3-chloropropyltrimethoxysilane in this study and iniferter groups were introduced by reacting the silica-bound chloropropyl groups with sodium *N,N*-diethyldithiocarbamate. Under the UV irradiation, it dissociates into surface grafted propyl radicals and dithiocarbamyl radical (DC) [23, 24]. The grafted propyl radical is reactive and initiates radical polymerization, while the DC radical is relatively stable and mainly reacts with growing radicals to

form a “dormant” species which reduces the concentration of free radicals to some extent. Additionally, molecular modelling studies were also carried out which assisted in choosing the suitable monomer for imprinting.

## Experimental section

### Materials

All chemicals and solvents were of analytical reagent grade, and used without further purification. Methacrylic acid (MAA) (99%), toluene, dimethyl formamide (DMF) were purchased from Loba chemie (Mumbai, India). Ethylene glycol dimethacrylate (EGDMA), silica gel (pore volume 60 Å, pore size 60 Å, 230–400 mesh size), 3-chloropropyltrimethoxysilane were purchased from Sigma Aldrich (Steinheim, Germany). Sodium *N,N*-diethyldithiocarbamate was purchased from MP Biomedicals, (LLC, France) and antipyrine (ANP), albendazole were purchased from Fluka (Steinheim, Germany). Aminopyrine was procured from HiMedia Laboratories Pvt. Ltd. (Mumbai, India), while 4-aminoantipyrine was purchased from Avra Synthesis Pvt. Ltd. (Hyderabad, India). Disodium hydrogen orthophosphate (anhydrous) and sodium dihydrogen orthophosphate (dehydrate) were obtained from Fischer Scientific. Other chemicals like methanol, acetic acid, aniline and ethanol were purchased from Merck (Mumbai, India).

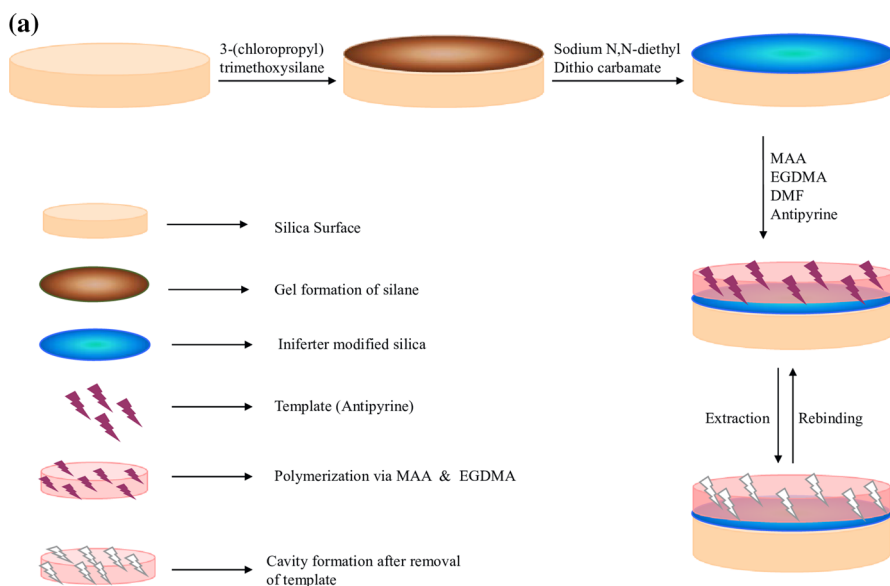
### Instruments

All electrochemical measurements were performed on a CHI 410B electrochemical workstation with three electrode system (a glassy carbon electrode, a platinum wire and Ag/AgCl electrode were used as working, counter and reference electrodes, respectively). Cyclic voltammograms of aqueous solution of ANP was run in potential range + 1.5 to – 0.5 V at scan rate of 0.1 Vs<sup>-1</sup>. The anodic current of ANP at 1.26 V in supporting electrolyte phosphate buffer (PBS) was recorded.

The IR spectra were recorded using JASCO FTIR 5300 in KBr from 400 to 4000 cm<sup>-1</sup>. Thermogravimetric analyses (TGA/DTA) were performed using Perkin Elmer instrument at 5 °C min<sup>-1</sup>. Atomic force microscopy (AFM) was performed by instrument Solver Next model of NT-MDT Company which is used for visualization and evaluation of surface dominant feature. Contact mode with soft silicon nitride tip, covered with reflective gold coating on the back side, was used to obtain the topography images. The AFM imaging was performed in air. The scanned area of the sample 5 nm × 5 nm and scan rate of AFM was 0.5 Hz. Elemental analyzer euro-vector—EA 3000 was used for elemental analysis.

### Grafting of iniferter on silica particle

Silica particles were modified by silanization with 3-chloropropyl trimethoxysilane. Activated silica particles (5.0 g) were refluxed for 8 h in solution of 3-chloropropyl trimethoxysilane (7.0 mL in 15 mL toluene), centrifuged subsequently and dried in



**Scheme 1** a Schematic representation for the preparation of surface-imprinted polymer of antipyrine; b mechanistic representation of imprinting pathway adopted for surface-imprinted polymer

vacuo at 60 °C after washing with toluene and stored in vacuo at room temperature (Scheme 1).

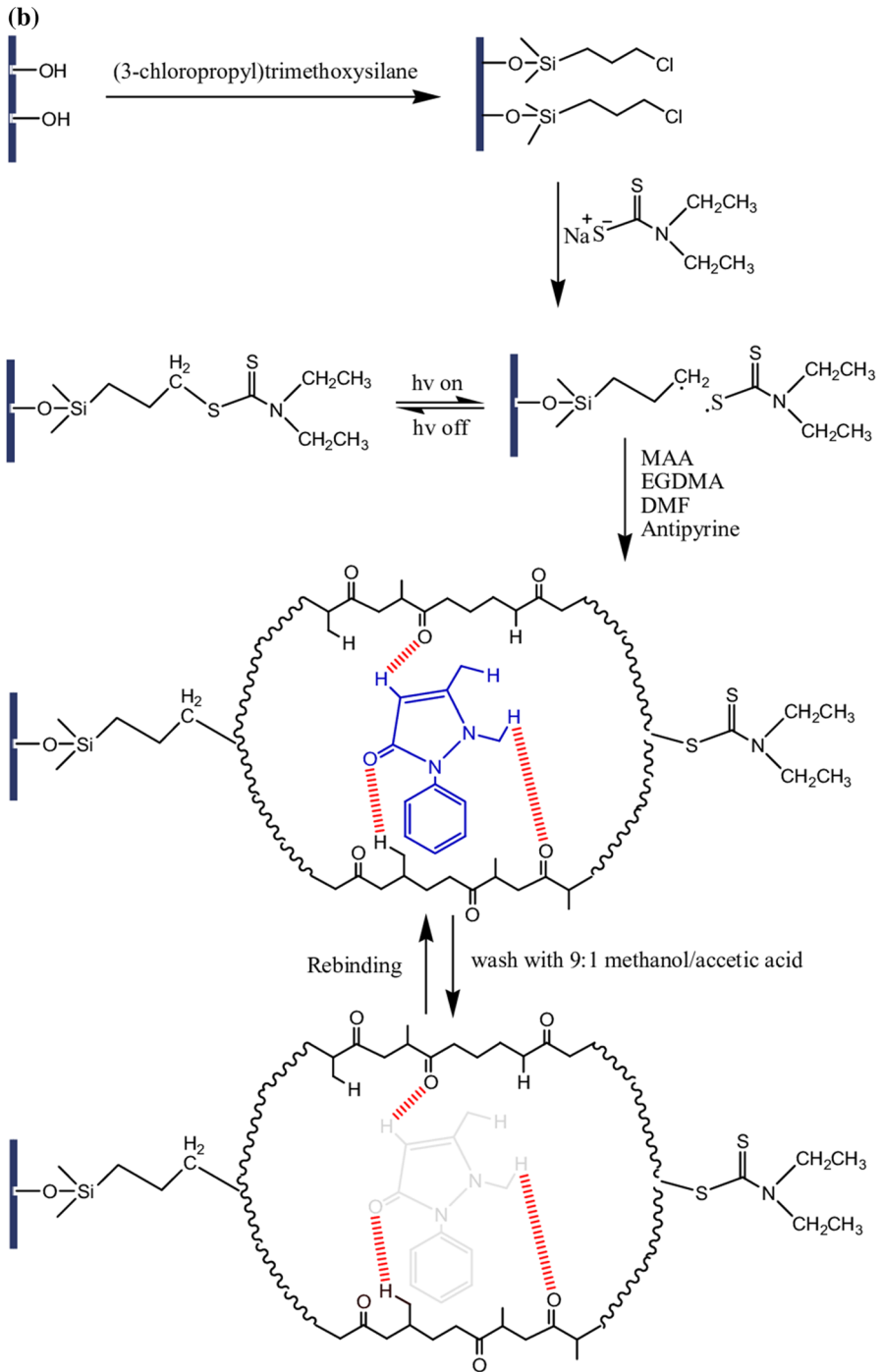
Iniferter was introduced by reaction of the silica-bound chloromethyl group with sodium *N,N*-diethyldithiocarbamate. Modified silica particles were treated with 0.3 M (1.63 g/25 mL ethanol) solution of sodium *N,N*-diethyldithiocarbamate for 24 h (Scheme 1). This iniferter-modified silica particles were washed and dried in oven for 2 h and stored under vacuum.

### Photografting of poly(methacrylic acid-*co*-ethyleneglycol dimethacrylate) onto the iniferter-modified silica

Iniferter-modified silica (1 g) was suspended in a solution of MAA (10 mM in 10 mL DMF), EGDMA (50 mM in 10 mL DMF) and the template ANP (1 mM in 10 mL DMF). This pre-polymerization mixture was irradiated in UV chamber for 6 h for polymerization. Thereafter, the obtained polymeric adduct were washed with toluene several times and stored for further use. Non-imprinted polymer (NIP) was prepared in the similar manner without template molecule.

### Extraction of template (ANP)

Antipyrine was extracted from a batch of 50 mg of imprinted silica particles with a solution of acetic acid and methanol (1:9, v/v) on continuous stirring. Extraction was monitored and verified by DPV measurements of extracted solutions. Removal



Scheme 1 continued

of analyte was confirmed by CV and DPV of extracted solution. ANP yields anodic current at 1.26 V in cyclic voltammogram [25]. Several analytical parameters like temperature, pH, extraction time, and volume of extracting solutions were optimized to obtain the best condition to extract antipyrine from imprinted matrix. The schematic representation of imprinting and removal of antipyrine from imprinted matrix is shown in Scheme 1.

### Rebinding and measurement of ANP with MIP and NIP

For the rebinding studies of ANP, a series of solutions with variable concentrations of ANP was prepared in aqueous solution (0.1–2.0 mM) and 2 mL of each solution was added to MIP-grafted silica particles (50 mg in a batch). Amount of ANP adsorbed by imprinted silica particles were estimated by DPV measurements before and after loading.

Limit of detection (LOD) was calculated as three times of standard deviation from blank measurement (in the absence of analyte ANP) divided by slope of calibration plot between ANP concentration and DPV current [26]. The extent of uptake of template molecules was estimated by DPV measurements of antipyrine before and after loading. All the measurements were made in triplicate.

### Cross-reactivity study

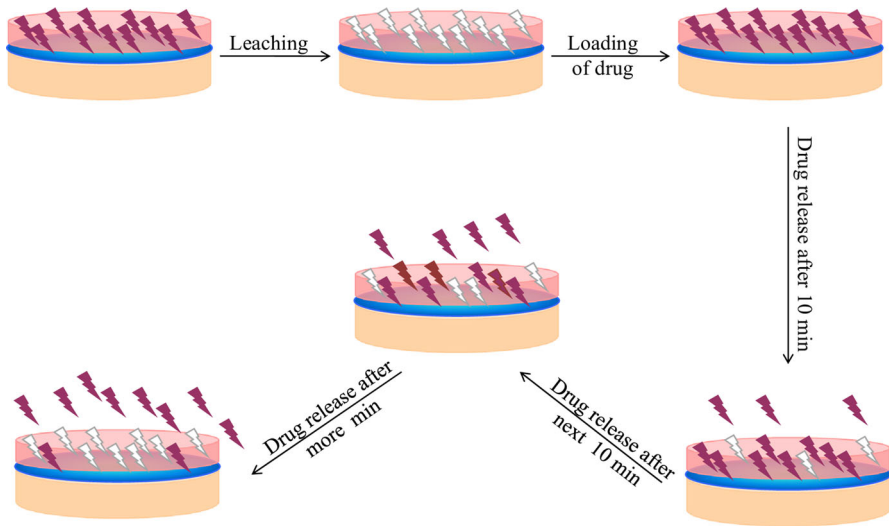
Selectivity of prepared MIP is studied further through several structural analogues of ANP with respect to functionally and structurally similar interfering agents, such as aniline, albendazole, ampyrone and aminopyrine. 50 mg of MIP-grafted silica was suspended in respective solutions of interferrants (5 mL of 0.1 mM aqueous solutions of each interferrant) for a period of 10 min. The extent of uptake of interferrant molecules was estimated by DPV measurements before and after loading.

### Drug loading by soaking procedure

Polymer grafted silica particles (0.1 g) were immersed in a solution of ANP (5 mM in 10 mL in deionized water) and soaked for 24 h at room temperature. During this time, the suspension was continuously stirred and then centrifuged and gently washed with deionized water to remove drug molecules physisorbed on surface (Scheme 2). 100 mg of imprinted silica particles was found to bind 2.8 mg of ANP as estimated by voltammetric measurements.

### Drug release from MIPs

Drug release experiments were carried out by transferring previously incubated drug loaded silica particles in 5 mL deionized water. The particles were repeatedly removed and transferred into 5 mL fresh deionized water at each fixed time interval. The released drug molecules were analysed by DPV measurements at 1.26 V. Effect of pH variation and ionic strength of release media was also studied. pH of the release media was varied by HCl/NaOH from 5 to 8. Ionic strength of release media



**Scheme 2** Schematic representation of drug delivery

is also a critical parameter affecting release kinetics. Here NaCl was chosen as model electrolyte to vary the ionic strength of release media (0.01–0.05 N).

## Calculations

Computer simulations were undertaken by Gaussian software (Gaussian 03) [27]. 3D chemical structures were generated using Gaussian View (Gauss View 4.1.2) [28]. The geometries of monomer, template and different complexes of ANP and MAA were optimized and binding energies (BEs) were calculated for respective complexes using density functional theory (DFT) at B3LYP/3-21G level with Gaussian 03 software [27]. BE of pre-polymerization complexes were calculated using equation

$$BE = E_{(\text{complex})} - [E_{(\text{template})} + nE_{(\text{monomer})}] \quad (1)$$

where  $E_{(\text{complex})}$  is the energy of template–monomer complex,  $E_{(\text{template})}$  is energy of ANP;  $E_{(\text{monomer})}$  is the energy of monomer and ‘ $n$ ’ is number of monomers. The basis set superposition error (BSSE) often substantially affects stabilization energies, was corrected by means of counterpoise method for complexes in gas phase

**Table 1** Binding energies of complexes in 1:1 mol ratio in solvents

Monomer + template complex in solvent	Binding energy $\Delta E$ (Kcal/Mol)
MAA + ANP in DMF	– 15.9387
MAA + ANP in DMSO	– 15.8132
MAA + ANP in Water	– 15.8132
MAA + ANP in $\text{CHCl}_3$	– 13.1149

[29]. Continuum polarized cavity model (CPCM) have been used for the evaluation of binding energy in solvents DMF, DMSO,  $\text{CHCl}_3$  and water (Table 1) [30].

## Results and discussion

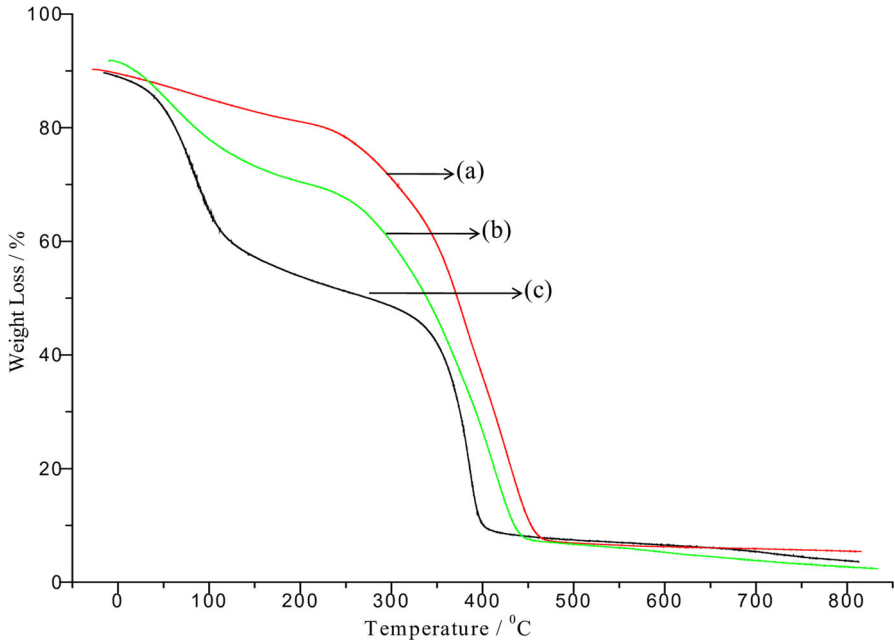
### Molecular modelling of interactions between monomer and ANP

Figure S1 shows the optimized structure of monomer and template molecule. Computation data (Table S1) indicates to facilitate ANP binding with MAA robustly, among the chosen monomers, thus making MAA an obvious choice for synthesis of ANP–MIP, as it is anticipated to confer high selectivity. Solvent (porogen) molecules compete with functional monomers for interactions with analyte molecules (ANP) during polymerization, thus the effect of solvent on imprinting was studied to understand molecular level interactions and identify the mode of interactions of ANP with monomer and solvent molecules (Table 1; Fig. S2). DMF (dielectric constant 36.70) was found to be suitable for imprinting ANP using MAA as functional monomer, since in DMF minimum binding energy of MAA and ANP interaction was found.

### MIP-carrier synthesis and physical characterization

ANP is a highly soluble drug substance with pH-independent dissolution due to its weak basic character [31]. Here, iniferter has been used for grafting MIP on silica surface, by grafting an iniferter on silica surface, it is expected that MIP can be formed only on the surface as polymerization takes place via active radical attached to silica surface, while the non-active radical is present in solution avoiding polymerization in solution. Grafting techniques have been recommended for imprinting, as grafting step is alienated from the imprinting step which is significant for creating high affinity binding sites, while maintaining other structural features of polymer matrix used for imprinting. Silica particles were sequentially functionalized with chloropropyl groups by silane coupling, followed by reacting with sodium *N,N*-dimethyl dithiocarbamate. MIPs were formed by photografting upon UV irradiation in the presence of ANP with MAA. Elemental analysis data for bare silica, iniferter-modified silica, MIP-grafted and NIP-grafted silica (Table S3) before and after coupling of the iniferter attests grafting of iniferter on silica particles. Regarding NIP- and MIP-modified silica; the organic content (C, H) was significantly higher showing the successful grafting of polymer chain on iniferter grafted silica particles. N content in NIP- and MIP-grafted silica particles is comparable, an insignificant change of  $\sim 0.3\%$  N from iniferter-modified silica is observed in both cases. Iniferter is the only molecule containing nitrogen here (apart from the template). Thermal stability of derivatives of silica, adduct, MIP, NIP, were investigated by TGA, as shown in Fig. 1. Overall degradation pattern is similar in all three cases, but solvent loss at  $\sim 100^\circ\text{C}$  is 40% in MIP before extraction (adduct), 25% in NIP and only 10% in MIP after extraction. Polymeric network grafted on silica starts degrading at  $\sim 250^\circ\text{C}$  and completely collapses at



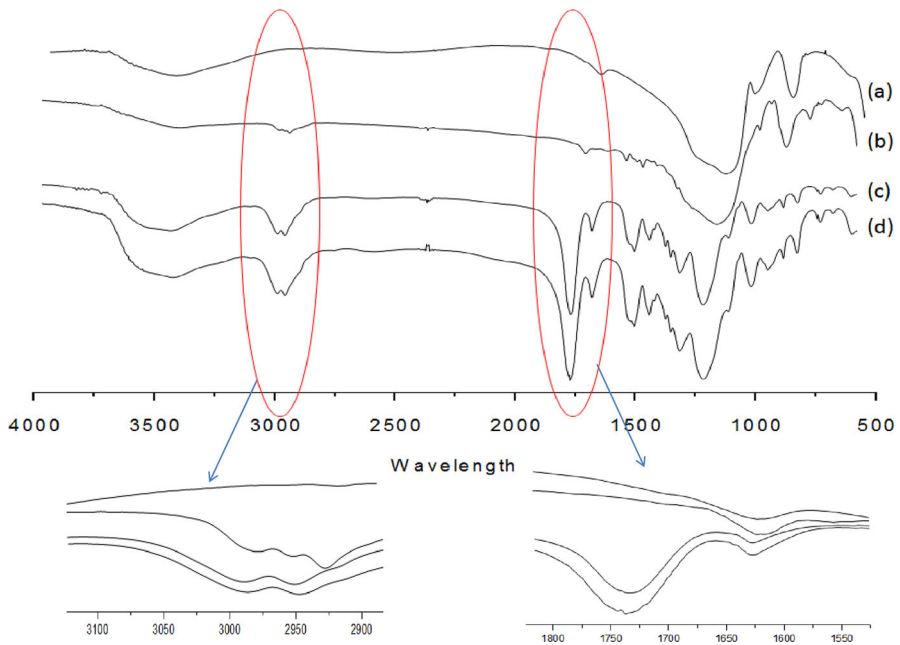


**Fig. 1** Thermogravimetric analysis measurements of the **a** molecularly imprinted polymer on modified silica, **b** non-imprinted polymer on modified silica and **c** adduct on modified silica

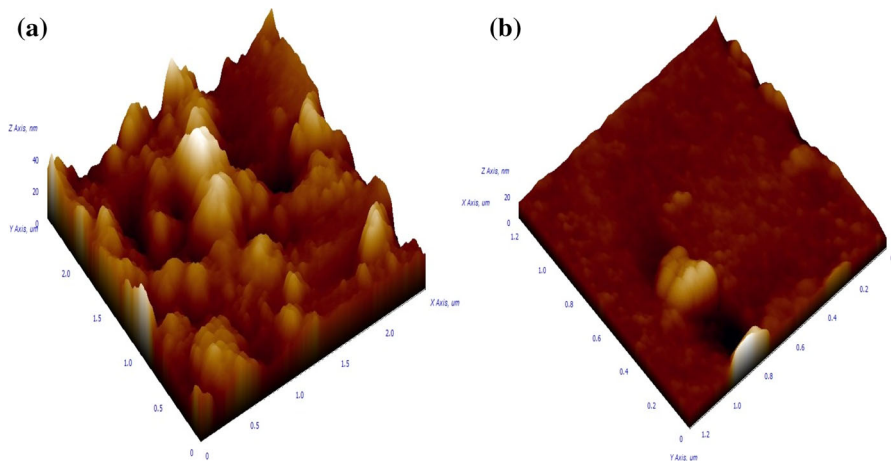
400–450 °C in each case. Similar degradation pattern of MIP-grafted and NIP-grafted silica is anticipated, as both are similar in composition, only difference being the absence of template molecule (here ANP) during growth of polymeric network in case of NIP.

Figure 2 shows FTIR spectrum of bare silica, iniferter-modified silica, MIP-grafted and NIP-grafted silica. Absorption band for bare silica is broad and intense at  $1200\text{--}1000\text{ cm}^{-1}$  (Si–O st). This band can be differentiating in each of the observed spectra of silica modification (Fig. 2 shown in box, inset 1). A broad band around  $2950\text{ cm}^{-1}$  (C–H st) ascribed to methyl and methylene groups is observed in curves b, c and d. Presence of this band in iniferter-modified silica (curve b) shows iniferter coupling at silica surface. In MIP and NIP spectra (curves c and d), an intense band is observed at around  $1730\text{ cm}^{-1}$  (inset 2), assigned to C=O stretching of functional monomer (MAA) and cross-linker (EGDMA) confirming grafting of polymer on silica particles.

Figure 3 shows AFM images of MIP- and NIP-grafted silica surface. Image of MIP shows the cavities created on imprinting, whereas NIP shows a smoother surface although the polymerization on both was carried out under similar conditions except using the template in polymerization mixture. It can be seen that roughness of MIP-coated electrode is enhanced manifold (Fig. S2) in comparison to NIP corroborating the imprinting mechanism proposed (Table S4).



**Fig. 2** FTIR spectra of **a** silica, **b** iniferter-modified silica, **c** molecularly imprinted polymer and **d** non-imprinted polymer



**Fig. 3** AFM images of **a** MIP-modified silica, **b** NIP-modified silica

### Rebinding/adsorption study of ANP on MIP

After polymerization, template molecules were extracted from the imprinting matrix. Removal of template (ANP) was confirmed by CV and DPV. ANP yields

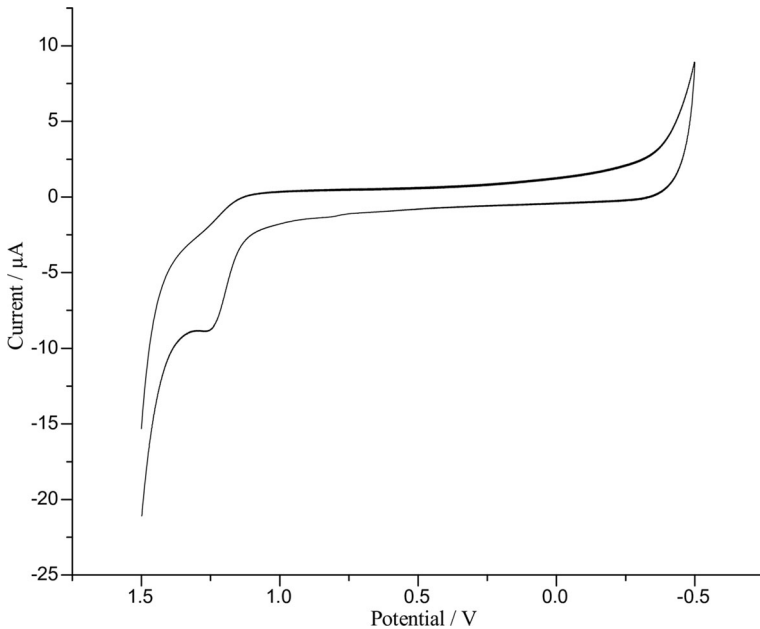


**Fig. 4** Cyclic voltammogram of antipyrine on glassy carbon electrode: potential range from 1.5 to  $-0.5$  with scan rate  $0.1 \text{ V s}^{-1}$  in PBS buffer

anodic current at 1.26 V in CV [25]. Figure 4 shows CV of ANP in a conventional electrochemical cell, using phosphate buffer (PBS) as supporting electrolyte.

Extracting parameters like number of washes, extraction time, extraction temperature and pH of extracting solution were optimized to obtain the best suited condition for extracting ANP from adduct (Fig. S3). For extracting ANP from adduct, the non-covalent interactions have to be broken up from imprinted network. At room temperature, extracting solvent was able to break the polymer–template interactions to release ANP from adduct network and form-imprinted cavities. Extraction of template was confirmed voltammetrically also (a peak at 1.26 V of ANP). Four washes with 3 mL aliquots of extracting solvent with constant mechanical stirring for 10 min at pH 4 was found to be sufficient for complete extraction of template ANP from polymeric network to craft specific-imprinted cavities (Fig. S3). Temperature of extracting solvent was found to have insignificant role in affecting extraction efficiency. The other set of parameters for rebinding the template (ANP) to imprinted cavities generated under above condition were also optimized. MIP takes 10 min to rebind the template molecule at pH 4 at 2 mM of ANP solution (Fig. S4).

Figure 5 shows a comparative study on the extent of ANP molecule being recovered by MIP and NIP at various concentrations of ANP. The non-specific bindings are responsible for template adsorption shown by NIP. These non-specific interactions are concentration-independent, as current does not appear to increase

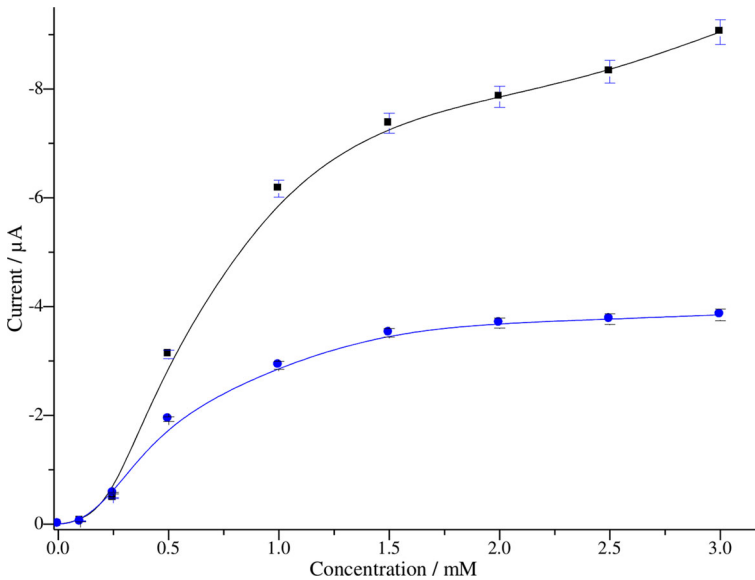


**Fig. 5** Changes in current in MIP and NIP at different concentrations of ANP (filled square: MIP; filled circle: NIP)

beyond 1 mM concentration of ANP. Although NIP is also comprised of similar components as MIP network but during network formation, increasing the potential for growing polymer chains with template binding complexes to reach a global energy minimum will lead to increased memorization of the chain conformation and enhance template binding.

Imprinting factor is widely used for assessing the efficiency of imprinting. Imprinting factor (IF) was used as a measure of the strength of interaction between the template and its corresponding functional monomer and was calculated according to the following equation:

$$IF = \frac{B_{MIP}}{B_{NIP}} \quad (2)$$

where  $B_{MIP}$  is the binding of analyte by molecularly imprinted polymer, while  $B_{NIP}$  is that of the non-imprinted polymer. Here ANP–MIP was found to have imprinting factor of 2.71 indicating the selectivity of MIP for ANP compared with NIP. Such data verifies the fact that the MIPs possessed good selectivity for ANP due to the fixed recognition cavities created during imprinting process which was propounded to be originating from ‘stoichiometric non-covalent interactions’, where the interaction during the polymerization was stoichiometric in nature [32–34]. Figure 6 shows the calibration plot for ANP–MIP, good linear relationship was obtained with  $R^2 = 0.9758$ . LOD in aqueous solution by ANP–MIP is calculated as  $0.448 \mu\text{g mL}^{-1}$  following standard analytical method [26].

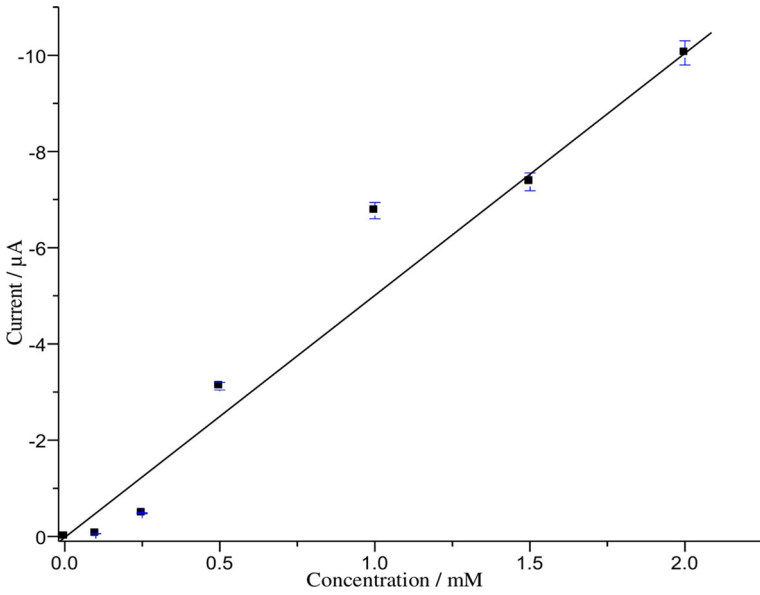


**Fig. 6** Calibration curve of MIP of iniferter-modified silica surface in response to various concentrations of template [ $R^2 = 0.9758$ ; RSD (%) = 3.01]

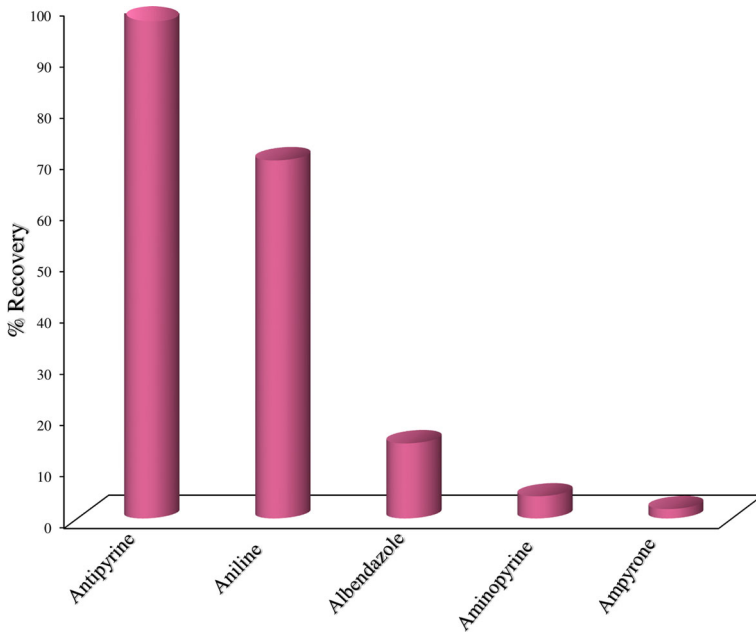


**Fig. 7** Changes in modified MIP current in response in various structural analogues (antipyrine; aniline; albendazole; aminopyrine; ampyrone)

## Selectivity study of MIP

Selectivity of prepared MIP is evaluated further through several structural analogues of ANP with respect to functionally and structurally similar interfering agents, such as aniline, albendazole, ampyrone and aminopyrine. The respective plots are shown in Fig. 7 illustrating the response of MIP under optimized parameters towards interferences. The template fits into imprinted cavity driven by complementary interactions followed by aligning of functional groups on MIP around template molecules conformational orientation. Binding for ANP was highest, but aniline also shows affinity for this MIP, as it is a major part of skeleton of antipyrine. Although albendazole, aminopyrine and ampyrone show insignificant binding which might be attributed to non-specific bindings. Since the binding of ANP (particularly aminopyrine and ampyrone) are relatively higher than those for aniline and albendazole, there may be a possibility of inter-anionic competition for receptor in MIP cavity, and ANP will have preference over other four analogues in terms of binding/uptake. Hence, the assay was analyte specific rather than group specific and thus suitable as a detection method for this analyte ANP.

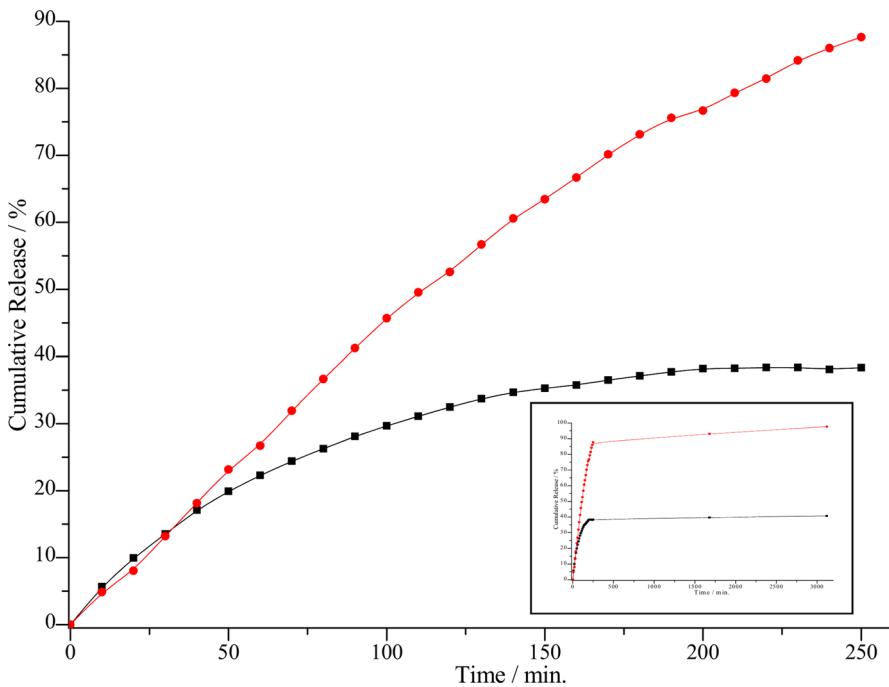


**Fig. 8** DPV response for drug release process of MIP and NIP at different time intervals after cumulative addition of current (filled circle: MIP; filled square: NIP)

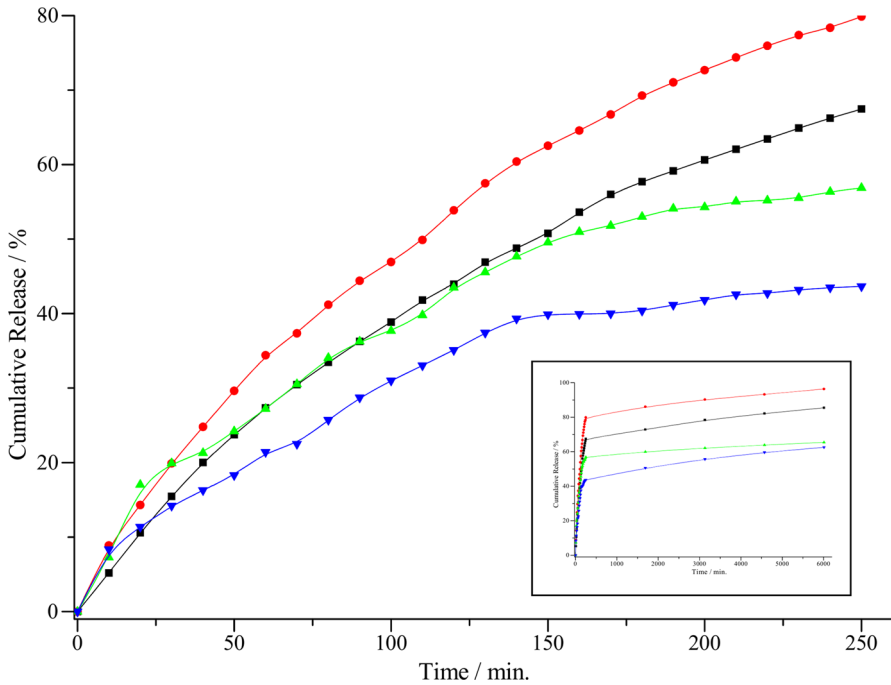


**Fig. 9** DPV response for drug release process of MIP at different time intervals after cumulative addition of current at varying pH (filled square: pH 5; filled circle: pH 6; filled triangle: pH 7; filled inverse triangle: pH 8)

### Drug loading and release studies

Drug loading was carried out by MIP carrier on incubating it with ANP in aqueous solution for 24 h. The carriers were then separated from the solution by centrifugation and dried. Release of ANP was studied, at predetermined time points, triplicate samples of the release media were withdrawn and replenished with fresh solvent to maintain a constant volume.

The release profile shows an initial steady release for almost 2 h which later on levelled out and sustained release for the studied time period, i.e., 52 h (Fig. 8). This sustained release is especially beneficial for drug delivery as per the need of diseased person. Imprinted polymers has the advantage of ‘sustained’ release not the ‘burst’ release, as observed in case of general purpose polymers including NIP [17, 35–38] (Fig. 8). Release behaviour was further studied under varying pH and ionic strength of release solution. Under acidic conditions, drug release was enhanced, but it slowed down under alkaline conditions. Drug molecules have a site (O atom) favourable for protonation and the charge developed could be delocalized over the ring thus providing an incentive to molecule to be released under acidic conditions. But in absence of any such structural incentive under alkaline conditions (Fig. 9), drug release is delayed. Effect of ionic strength is also studied for drug

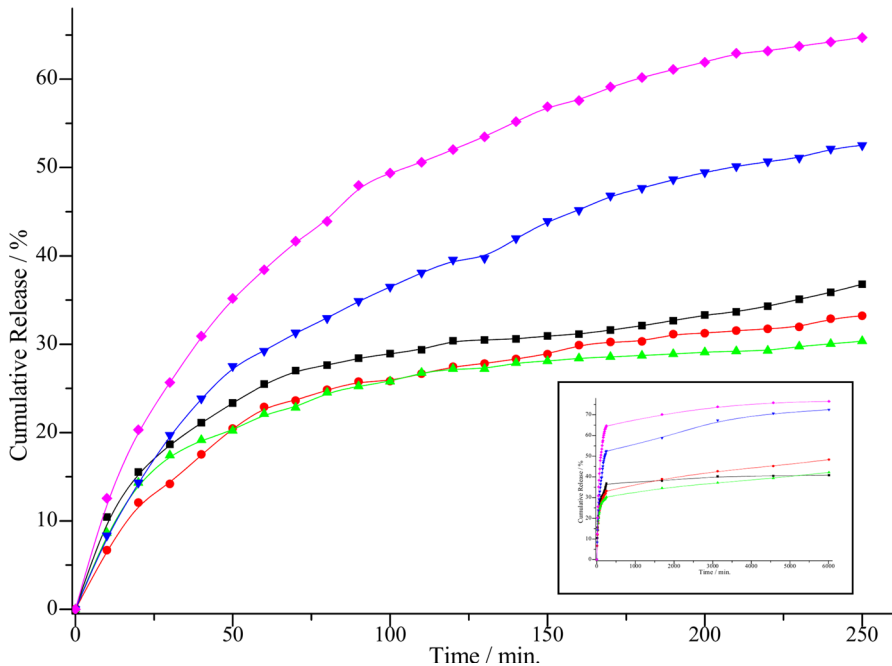


**Fig. 10** DPV response for drug release process of MIP at different time intervals after cumulative addition of current at varying ionic strengths (filled square: 0.01 N NaCl; filled circle: 0.02 N NaCl; filled triangle: 0.03 N NaCl; filled inverse triangle: 0.04 N NaCl; filled star: 0.05 N NaCl)

release. A little effect is observed on increasing ionic strength from 0 to 0.03 N NaCl (Fig. 10) but release was enhanced manifold on further increasing the concentration of NaCl to 0.05 N. Addition of water molecules provides competition to solvent molecules entering into polymeric matrix in lieu of drug molecules. More salt molecules enhance the osmosis of salt solution. It is the net effect of salt imbibed within the imprinted matrix and solvent molecules also moving into the polymeric matrix to replace drug molecules. Hence under electrolyte stress, release behaviour will change under biological environment.

## Conclusion

An iniferter-mediated surface-imprinted polymer via photo grafting was successfully grafted on silica particles. Molecular modelling through DFT calculations accomplished the design of best suited experimental components like functional monomer and porogen for imprinting. ANP–MIP-grafted silica particles were characterized by elemental analysis, FTIR, thermogravimetric analysis, AFM images and other extraction and imprinting parameters. NIP-grafted silica particles were also tested for validation of selectivity and specificity of ANP–MIP. Additionally, experiments with structural analogues also attested the selectivity of ANP–MIP. Thus, fabricated ANP–MIP was utilized as drug delivery instrument for



sustained release of ANP as drug under various stress factors such as ionic strength, pH.

**Acknowledgements** Authors acknowledge Department of Chemistry, Banaras Hindu University for AFM analysis. AK acknowledges UGC and BHU for university research fellowship. Financial assistance from DST, New Delhi is acknowledged (Grant no. EMR/2016/005245).

## References

1. Brodie BB, Axelrod J (1950) The fate of antipyrine in man. *J Pharmacol Exp Ther* 98:97–104
2. Hoberman A, Paradise JL, Reynolds EA, Urkin J (1997) Efficacy of Auralgan for treating ear pain in children with acute otitis media. *Arch Pediatr Adolesc Med* 151:675–678
3. Marmura MJ, Stephen SD, Schwedt TJ (2015) The acute treatment of migraine in adults: the American Headache Society evidence assessment of migraine pharmacotherapies. *Headache* 55:3–20
4. Zuehlke S, Duennbier U, Heberer T (2007) Investigation of the behavior and metabolism of pharmaceutical residues during purification of contaminated ground water used for drinking water supply. *Chemosphere* 69:1673–1680
5. Wiegel S, Aulinger A, Brockmeyer R, Harms H, Löffler J, Reincke H, Schmidt R, Stachel B, Von Tümpling W, Wanke A (2004) Pharmaceuticals in the river Elbe and its tributaries. *Chemosphere* 57:107–126
6. Reddersen K, Heberer T, Dünnbier U (2002) Identification and significance of phenazone drugs and their metabolites in ground- and drinking water. *Chemosphere* 49:539–544
7. Cai M, Zhang L, Qi F, Feng L (2013) Influencing factors and degradation products of antipyrine chlorination in water with free chlorine. *J Environ Sci* 25:77–84
8. Sakamoto JH, van de Ven AL, Godin B, Blanco E, Serda RE, Grattoni A, Ziemys A, Bouamrani A, Hu T, Ranganathan SI, De Rosa E, Martinez JO, Smid CA, Buchanan RM, Lee S-Y, Srinivasan S, Landry M, Meyn A, Tasciotti E, Liu X, Decuzzia P, Ferrari M (2010) Enabling individualized therapy through nanotechnology. *Pharmacol Res* 62:57–89
9. Lulinski P (2017) Molecularly imprinted polymers based drug delivery devices: a way to application in modern pharmacotherapy. *Mater Sci Eng C* 76:1344–1353
10. Wulff G, Gross T, Schonfeld R (1997) Enzyme models based on molecularly imprinted polymers with strong esterase activity. *Angew Chem Int Ed* 36:1962–1964
11. Toorisaka E, Yoshida M, Uezu K, Goto M, Furusaki S (1999) Artificial biocatalyst prepared by the surface molecular imprinting technique. *Chem Lett* 28:387–388
12. Mosbach K, Ramstom O (1996) The emerging technique of molecular imprinting and its future impact on biotechnology. *Nat Biotechnol* 14:163–170
13. Vidyasankar S, Dhal PK, Plunkett SD, Arnold FH (1995) Selective ligand-exchange adsorbents prepared by template polymerization. *Biotechnol Bioeng* 48:431–436
14. Kempe M, Mosbach K (1995) Molecular imprinting used for chiral separations. *J Chromatogr A* 694:3–13
15. Saha D, Warren KE, Naskar AK (2014) Controlled release of antipyrine from mesoporous carbons. *Microporous Mesoporous Mater* 196:327–334
16. Salonen J, Laitinen L, Kaukonen AM, Tuura J, Bjorkqvist M, Heikkila T, Vaha-Heikkila K, Hirvonen J, Lehto V-P (2005) Mesoporous silicon microparticles for oral drug delivery: loading and release of five model drugs. *J Control Release* 108:362–374
17. Goscianska J, Olejnik A, Nowak I (2017) APTES-functionalized mesoporous silica as a vehicle for antipyrine-adsorption and release studies. *Colloids Surf A* 533:187–196
18. Sangalli ME, Maroni A, Zema L, Busetti C, Giordano F, Gazzaniga A (2001) In vitro and in vivo evaluation of an oral system for time and/or site-specific drug delivery. *J Control Release* 73:103–110
19. Gazzaniga A, Sangalli M, Giordano F (1994) Oral Chronotopic<sup>®</sup> drug delivery systems: achievement of time and/or site specificity. *Eur J Pharm Biopharm* 40:246–250
20. Gazzaniga A, Iamartino P, Maffione G, Sangalli ME (1994) Oral delayed-release system for colonic specific delivery. *Int J Pharm* 108:77–83
21. Gazzaniga A, Busetti C, Sangalli ME, Moro L, Giordano F (1995) Oral delayed-release system for colonic specific delivery. *Int J Pharm* 5:83–88

22. Yang G, Wang D, Li Z, Zhou S, Chen Y (2003) Adsorption isotherms on aminoantipyrine imprinted polymer stationary phase. *Chromatographia* 58(1):53–58
23. Otsu T, Yoshida M (1982) Role of initiator–transfer agent–terminator (iniferter) in radical polymerization: polymer design by organic disulfides as iniferters. *Macromol Rapid Commun* 3:127–132
24. Otsu T, Matsunaga T, Doi T, Matsumoto A (1995) Features of living radical polymerization of vinyl monomers in homogeneous system using *N, N*-diethyldithiocarbamate derivatives as photoiniferters. *Eur Polym J* 31:67–78
25. Calderera-Moore M, Peppas NA (2009) Micro- and nanotechnologies for intelligent and responsive biomaterial-based medical systems. *Adv Drug Deliv Rev* 61:1391–1401
26. Skoog DA, Holler FT, Nieman TA (1998) Principles of instrumental analysis, 5th edn. Harcourt Brace College Publishers, Florida, pp 13–14
27. Frisch MJ, Trucks GW, Schlegel HB, Scuseria GE., Robb MA, Cheeseman JR, Montgomery JA, Vreven JT, Kudin KN, Burant JC, Millam JM, Iyengar SS, Tomasi J, Barone V, Mennucci B, Cossi M, Scalmani G, Rega N, Petersson GA, Nakatsuji H, Hada M, Ehara M, Toyota K, Fukuda R, Hasegawa J, Ishida M, Nakajima T, Honda Y, Kitao O, Nakai H, Klene M, Li X, Knox JE, Hratchian HP, Cross JB, Bakken V, Adamo C, Jaramillo J, Gomperts R, Stratmann RE, Yazyev O, Austin AJ, Cammi R, Pomelli C, Ochterski JW, Ayala PY, Morokuma K, Voth GA, Salvador P, Dannenberg JJ, Zakrzewski VG, Dapprich S, Daniels AD, Strain MC, Farkas O, Malick DK, Rabuck AD, Raghavachari K, Foresman JB, Ortiz JV, Cui Q, Baboul AG, Clifford S, Cioslowski J, Stefanov BB, Liu G, Liashenko A, Piskorz P, Komaromi I, Martin RL, Fox DJ, Keith T, Al-Laham MA, Peng CY, Nanayakkara A, Challacombe M, Gill PMW, Johnson B, Chen W, Wong MW, Gonzalez C, Pople JA (2004) Gaussian03 Revision D01. Gaussian Inc, Wallingford
28. Dennington R, Keith T, Millam J (2007) GaussView 4.1. Semichem, Inc. Shawnee Mission
29. Boys SF, Bernardi FD (1970) The calculation of small molecular interactions by the differences of separate total energies. Some procedures with reduced errors. *Mol Phys* 19:553–566
30. Cossi M, Barone V, Cammi R, Tomasi J (1996) Ab initio study of solvated molecules: a new implementation of the polarizable continuum model. *Chem Phys Lett* 255(4–6):327–335
31. Salonen J, Laitinen L, Kaukonen AM, Tuura J, Björkqvist M, Heikkilä T, Vähä-Heikkilä K, Hirvonen J, Lehto V-P (2005) Mesoporous silicon microparticles for oral drug delivery: loading and release of five model drugs. *J Control Release* 108(2):362–374
32. Sellergren B, Lepistö M, Mosbach K (1988) Highly enantioselective and substrate-selective polymers obtained by molecular imprinting utilizing noncovalent interactions. NMR and chromatographic studies on the nature of recognition. *J Am Chem Soc* 110:5853–5860
33. Mosbach K, Haupt K (1998) Some new developments and challenges in non-covalent molecular imprinting technology. *J Mol Recognit* 11:62–68
34. Zhang H, Ye L, Mosbach K (2006) Non-covalent molecular imprinting with emphasis on its application in separation and drug development. *J Mol Recognit* 19:248–259
35. Norell MC, Andersson HS, Nicholls IA (1998) Theophylline molecularly imprinted polymer dissociation kinetics: a novel sustained release drug dosage mechanism. *J Mol Recognit* 11:98–102
36. Cunliffe D, Kirby A, Alexander C (2005) Molecularly imprinted drug delivery systems. *Adv Drug Deliv Rev* 57:1836–1853
37. Huang X, Brazel CS (2001) On the importance and mechanisms of burst release in matrix-controlled drug delivery systems. *J Control Release* 73:121–136
38. Zaidi SA (2016) Molecularly imprinted polymers as drug delivery vehicles. *Drug Deliv* 23:2262–2271